Ecotoxicology and Environmental Safety 168 (2019) 212–220

Contents lists available at ScienceDirect

Ecotoxicology and Environmental Safety

journal homepage: www.elsevier.com/locate/ecoenv

Formation of iron plaque in the roots of *Spartina alterniflora* and its effect on the immobilization of wastewater-borne pollutants

Qiqiong Zhang, Zhongzheng Yan*, Xiuzhen Li, Yan Xu, Xiangli Sun, Qiuyao Liang

State Key Laboratory of Estuarine and Coastal Researches, East China Normal University, Shanghai, China

ARTICLE INFO

Keywords:
Spartina alterniflora
Wastewater
Heavy metals
Iron plaque
Nitrogen
Phosphorus

ABSTRACT

Iron plaque (IP) plays an important role in the absorption of heavy metals (HMs) and nutrients in wetland plants. The present study aims to investigate the effect of IP in *Spartina alterniflora* on the immobilization of wastewater borne HMs and nutrients. The physiological responses and effect of IP formation on the uptake of HMs, nitrogen (N), and phosphorus (P) were studied in *S. alterniflora* subjected to different synthetic wastewater (SW) levels and waterlogging durations. Results showed that IP formed in roots of *S. alterniflora* increased significantly with increasing SW concentration but decreased under prolonged waterlogging. Increasing the waterlogging time enhanced the alcohol dehydrogenase activity and the ethylene content in the roots of *S. alterniflora*. HMs including Cu, Pb, and Cr, did not significantly accumulate in the IP, despite that the IP content increased with the increasing of SW levels. The SEM–EDX analysis revealed that IP formed on the surface of *S. alterniflora* did absorb HMs such as Cu, Zn, and Cr. At a fixed level of SW, the amount of HMs that accumulated in the DCB extract was substantially proportional to the IP concentration in the root. Increasing of the SW level enhanced the accumulation of P in the leaves and roots of *S. alterniflora*. In conclusion, IP formed on *S. alterniflora* helped immobilize SW pollutants, including HMs and P, and the formation of IP and its effect on pollutant immobilization were influenced by the waterlogging conditions.

1. Introduction

Due to the development of industrial and agricultural activities and urbanization, million tons of industrial and domestic sewage discharges, commercial harbors, iron and steel mill constructions have caused severe pollution in estuary wetlands of Yangtze River delta (Yang et al., 2012; Wang et al., 2015). Excessive discharge of elements, such as nitrogen (N) and phosphorus (P), into coastal estuarine areas has induced massive eutrophication problems (Chai et al., 2006; Yang et al., 2012). Heavy metals (HMs) in wastewater accumulate on wetlands through absorption and coprecipitation (Chibuike and Obiora, 2014). Salt marsh plants, such as *Spartina alterniflora* and *Phragmites australis*, occupy vast regions of the Yangtze River estuary and are vulnerable to anthropogenic pressures, including increased environmental pollution (Anjum et al., 2014). Salt marsh plants can extract, accumulate, or stabilize various metal pollutants and significantly reduce metal availability in sediments by promoting system auto-remediation through phytoremediation (Weis and Weis, 2004; Chai et al., 2013; Anjum et al., 2014).

Tidal inundation exerts fundamental influences on the distribution and survival of salt marsh plants in coastal wetlands (Duarte et al., 2015; Thakur et al., 2016). Wetland plants can form extensive aerenchyma tissues in roots and aerial parts to cope with flooding stress (Yamauchi et al., 2018). The aerenchyma provides a low-resistance pathway for rapid flux of oxygen (O_2) from the aerial plant parts to the roots. Excessive O_2 and other oxidizing substances diffuse from the roots to the surroundings to change the redox environment of the rhizosphere; this process is called radial oxygen loss (ROL) (Smith and Luna, 2013). ROL not only creates a local oxidative environment for the rhizosphere of wetland plants but also oxidizes Fe^{2+}/Mn^{2+} in porewater and leads to the formation of Fe/Mn plaque on the root surface of wetland plants (Otte et al., 1989). Tidal flat sediments contain abundant metals, such as Fe and Mn, whose valence states are affected by the redox potential of the sediments and the changes between trivalence and bivalence states (Khan et al., 2016). Fe^{3+}/Mn^{3+} oxidants (hydroxide) precipitated on wetland plant roots can immobilize wastewater-borne pollutants and enhance their removal. Periodic flooding of tidal flats changes the redox potential and pH of sediments, thereby altering the valence states of Fe and Mn and affecting the formation of iron plaque (IP) and the biological effectiveness of HMs. Previous research showed that waterlogging can affect the formation of IP by increasing the root ROL rate (Jackson and Armstrong, 1999). Nevertheless,

* Correspondence to: State Key Laboratory of Estuarine and Coastal Researches, East China Normal University, 3663 Zhongshan Rd North, Shanghai, China.
E-mail address: zzyan@sklec.ecnu.edu.cn (Z. Yan).

https://doi.org/10.1016/j.ecoenv.2018.10.072
Received 8 June 2018; Received in revised form 18 October 2018; Accepted 20 October 2018
Available online 30 October 2018

extending the flooding time may inhibit the ROL of the roots because of cell aging and increased ROL barrier (Xu et al., 2013). The increase in the root porosity is generally derived from root tissue aging and cavity, which are related to nutrient levels in root surroundings, plant growth stage, and resistance of plants under stressful environments (Shimamura et al., 2003; Striker, 2012). Under anaerobic conditions, the roots can promote ethylene synthesis, such that they will accelerate the aging of cells and the formation of aerenchyma tissues to some extent (Takahashi et al., 2014).

Studies have demonstrated IP formation in the roots of most wetland plants, such as *Aster tripolium* (Otte et al., 1989), *Oryza sativa* (Lee et al., 2013), *Typha latifolia* (Ye et al., 2001) and *Bruguiera gymnorrhiza* (Pi et al., 2011). IPs are mainly consisted of amorphous and crystalline iron oxyhydroxides, which can affect the uptake and translocation of nutrients and HMs through combination and coprecipitation because of their large surface area with positive and negative charges (Khan et al., 2016). Scholars have focused on understanding of the role of IP in element translocation and achieved contrasting results. IP facilitates the uptake of elements by acting as a "reservoir." When plants lack nutrients, IP will activate the reserved elements and promote plant uptake via its strong affinity to the nutrient (Zhang et al., 1999). Other researchers regard IP as "barrier" that inhibits the uptake of elements; moreover, iron oxides in IP are thought to immobilize HMs and other anions to restrain their transportation (Pi et al., 2011; Mei et al., 2014; Yang et al., 2014; Sebastian and Prasad, 2016). As a typical perennial wetland plant with deep roots and high aboveground biomass, *S. alterniflora* is believed to have a potential for phytoremediation of pollutants in estuarine wetland due to its ability in the phytostabilization of HMs and nutrients (Weis and Weis, 2004). However, to date, still very little is known on the formation of IP on the root surface of *S. alterniflora* and its role in the uptake of HMs and nutrient elements under periodic flooding conditions. The present study conducted a controlled experiment in a climate chamber and aimed to investigate the formation of IP under the influences of different synthetic wastewater (SW) levels and waterlogging durations. The significance of IP formation on the immobilization of HMs and nutrients was also evaluated.

2. Materials and methods

2.1. Experimental setup

Healthy seedlings of *S. alterniflora* with comparable sizes (about 50 cm in height) were collected from the Nanhui wetland of Shanghai in May 2017. The collected seedlings were grown in 24 polypropylene (PP) pots [32.5 cm (L) × 14 cm (W) × 22.5 cm (H)]. Each pot contained four seedlings and 18 kg of sediments collected from the ambient environment in the Nanhui wetland. The texture and other physiochemical properties of the sediments are summarized in Table S1. The pots were placed in an artificial climate chamber with diurnal temperature ranging from 20 °C to 30 °C, a relative humidity of 70% ± 5%, a light intensity of 800–1400 μmol photons m^{-2} s^{-1} with a 12:12 light:dark photoperiod.

After 14 days of rejuvenation, all the pots were transferred into a flooding device (Fig. 1). The flooding device mainly includes two parts: a water tank [52 cm (L) × 38 cm (W) × 28 cm (H)] and a bucket (19 L). PP pots planted with *S. alterniflora* were placed in the upper water tank, and the treatment solutions were placed in the lower bucket. The treatment solutions in the lower bucket were pumped into the upper water tank by a sinking pump and kept in the upper water tank for a given period of time to simulate the periodic tide of the Yangtze river estuary. The solution in the upper tank was drained to the lower water tank through a valve to complete a waterlogging cycle. The pots in the water tanks received waterlogging twice per day.

Twelve pots of *S. alterniflora* seedlings were chosen to test the effect of different levels of SW on physiology and IP formation in *S. alterniflora*. The pots were randomly divided into four groups, with three replicates each. One group received salt water (10‰ NaCl) and served as control. The three other groups were treated with different SW levels, namely, 5, 10, and 20 SW. The 1 × SW solution was prepared according to the Shanghai municipal sewage concentration and Chinese sewage discharge standard by using 0.5 mg L^{-1} NO_3^-–N, 25 mg L^{-1} NH_4^+–N, 19.5 mg L^{-1} dissolved organic N, 5 mg L^{-1} PO_4^{3-}–P, 2 mg L^{-1} Cu^{2+}, 5 mg L^{-1} Zn^{2+}, 1 mg L^{-1} Pb^{2+}, 0.5 mg L^{-1} Cr^{6+}, 30 mg L^{-1} Fe^{3+}, and 10‰ NaCl. The 5SW, 10SW and 20SW treatments were prepared using 5, 10, and 20 times of 1 × SW, respectively. All the treatments were flooded with the treatment solution as described above to a height of 5 cm above the soil surface twice a day for 8 h per day in total (7 a.m. to 11 a.m. and 7 p.m. to 11 p.m.) to simulate the semi-diurnal tides of the Yangtze estuary.

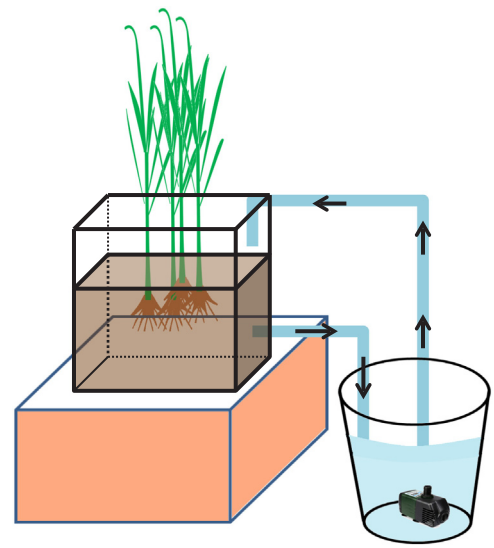

Fig. 1. The diagram of the waterlogging systems in this study.

Four other groups were used to test the effect of different times of waterlogging on plant physiology, IP formation, and pollutant uptake and translocation in *S. alterniflora*. The four groups were treated with 10 SW as described above and subjected to different durations of waterlogging every day: namely, 0 h + 10SW (normal irrigation to keep the soil wet), 4 h + 10SW (flooding from 7 a.m. to 9 a.m. and from 7 p.m. to 9 p.m.), 8 h + 10SW (flooding from 7–11 a.m. and from 7–11 p.m.), and 12 h + 10SW (flooding from 7 a.m. to 1 p.m. and from 7 p.m. to 1 a.m. of the next day). One group received only salt water (10‰ NaCl) and served as control. All the treatment solutions were replenished every 7 days until the end of the experiments.

Samples were obtained 45 days after the experimental treatment. One plant in each replicate was selected for root IP extraction and porosity measurement. During sampling, the plant was carefully removed from the pot. The residual soil attached to the root was first washed with tap water and rinsed three times with deionized water. After drying with absorbent paper, a piece of 8–12 cm lateral root was selected and cut into 1 cm pieces. About 0.1 g of the root piece was used for IP extraction, and another 0.1 g was used for root porosity determination. The root sample was fixed with FAA for subsequent environmental scanning electron microscopy observation of IP distribution. The roots, stems, and leaves of the remaining plants were separated, crushed, mixed thoroughly, rapidly frozen in liquid N, and stored at −80 °C until further analyses. Soil samples of each replicate were also collected, dried, and used for determination of HMs as well as N and P.

2.2. Measurement

2.2.1. Root porosity

Root porosity was measured using a pycnometer according to the method described by Jensen et al. (1969). The lateral roots of *S. alterniflora* were rinsed thoroughly with deionized water to remove adhering sediments. The roots were cut into segments with length of about 2 cm. About 0.1 g of the root segments were weighed in a 25 mL pycnometer. The pycnometer was filled with distilled water and weighed on an analytical balance. The weight was recorded as W_{r+w}. The root was removed from the pycnometer, dried with absorbent paper, and immediately weighed on the analytical balance. The weight was recorded as W_r. The root segments were ground into paste with a mortar and returned entirely to the pycnometer. The pycnometer bottle was filled with distilled water and weighed again. The weight was recorded as W_h. The weight of the pycnometer filled with water only was recorded as W_w. All measurements were carried out at room temperature (25 °C). Root porosity was calculated according to the equation below:

$$\% \text{ Porosity} = 100(W_h - W_{r+w})/(W_w + W_r - W_{r+w})$$

2.2.2. IP content and HM concentration in IP

IP on the root surface was extracted by dithionite–citrate–bicarbonate (DCB) method according to Taylor and Crowder (1983). About 0.1 g of fresh lateral root was agitated in 10 mL of precold DCB solution containing 0.3 mol L^{-1} sodium citrate ($Na_3C_6H_5O_7 \cdot 2H_2O$), 1 mol L^{-1} sodium bicarbonate ($NaHCO_3$), and 60 g L^{-1} of sodium dithionite ($Na_2S_2O_4$) at 25 °C for 3 h. The DCB extract was poured into 25 mL volumetric flask, and the roots were rinsed three times with deionized water. The washes were combined up to a constant volume. The concentrations of Fe, Cu, Zn, Pb, and Cr in the solution were determined by inductively coupled plasma–atomic emission spectrometry (ICP-AES, ICAP-7400, Thermo Fisher Inc., USA)

2.2.3. Concentrations of HMs, N, and P in plant tissues

The concentrations of HMs in different plant parts were determined by wet digestion method. After sample collection, all the plant parts were dried at 60 °C to a constant weight and ground. About 0.2 g of the dried plant tissue was digested in a polyfluortetraethylene (PTFE) beaker containing 10 mL of nitric acid, 5 mL of hydrofluoric acid, and 5 mL of perchloric acid. The PTFE beaker was heated on an electric hot plate at 200 °C for 3 h. During the digestion, the lid of the PTFE beaker was kept covered to avoid the splashing of the digest. After digestion, the remnant in the beaker was dissolved and washed three times with 5 mL of 1% nitric acid. The washes were combined in a volumetric flask and added with deionized water up to 25 mL volume. The concentration of HMs was determined by ICP-AES (ICAP-7400, Thermo Fisher Inc., USA). Certified reference material (CRM) of carrot from GBW10047 (GSB-25) was used for quality control. The average recovery rates for Cu, Zn, Pb, and Cr in CRM were 96.02% ± 3.69%, 90.19% ± 5.40%, 105.02% ± 13.31%, and 93.06% ± 7.61%, respectively.

The contents of carbon (C) and N in the plant tissues were determined by a CHN analyzer (Vario Macro CNS, Elemental Analyzer, Germany). P content in the plant tissues was determined by molybdenum (Mo)–antimony (Sb) colorimetric method according to Tsang et al. (2007). An aliquot of 0.1 g of dried plant tissue was digested in 4 mL of concentrated sulfuric acid (H_2SO_4) overnight and heated on an electric hot plate at 200 °C until the solution becomes homogeneous. The solution was added with hydrogen peroxide (H_2O_2) until it became colorless. The solution was made up to a constant volume of 50 mL, diluted five times, and added with 2.5 mL of Mo–Sb–Vc to determine absorbance at 700 nm. The recovery rate for P is 92.19% ± 1.279%.

2.2.4. ADH activity and ETH content in the root of S. alterniflora

ADH activity and ETH concentration in the plant roots were determined using an enzyme-linked immunosorbent assay kit (Rapidbio, USA) according to the instructions of the manufacturer. About 0.1 g of the root sample was homogenized with 1.5 mL of 10 × phosphate buffer consisting of 137 mmol L^{-1} NaCl, 2.7 mmol L^{-1} KCl, 8 mmol L^{-1} Na_2HPO_4, and 1.46 mmol L^{-1} KH_2PO_4. The homogenates were centrifuged at 12,000 rpm for 5 min at 4 °C, and the supernatant was used for determination. The standards of ADH or ETH and the samples were placed into microplate wells with horseradish peroxidase (HRP)-conjugated ADH or ETH and then incubated. A competitive inhibition reaction was started between ADH or ETH and HRP-conjugated ADH or ETH with the precoated antibody specific for ADH or ETH. The optical density of the wells was read at 450 nm by using a microplate reader (Infinite 200 Pro, Tecan Group Ltd., Switzerland). The detection limit of this assay for ADH and ETH were 0.1 U mL^{-1} and 10.0 pmol L^{-1}, respectively.

2.2.5. Scanning electron microscopy (SEM) and energy-dispersive X-ray (EDX) microanalysis

The collected root samples were washed by tap water and rinsed three times with deionized water. The lateral root was fixed in 2.5% glutaraldehyde in 0.1 mmol L^{-1} phosphate buffer (pH 7.2) for 8 h and dehydrated by ethanol. IP in the root of *S. alterniflora* was observed by SEM. During the observation, root specimens were mounted on aluminum mounting stubs, coated with gold–palladium, and visualized with SEM-EDX (JSM-6390A, JEOL Ltd., Japan) under 20 kV accelerating voltage and data collection time of 60 s. Fe and HMs present on the surface and transverse section of the root was localized by X-ray mapping through EDX analysis.

2.3. Statistical analyses

The mean and standard deviations of the three replicates for each treatment were calculated. Parametric one-way ANOVA and post-hoc multiple comparison (Tukey's test) were conducted to determine significant differences in different parameters after treatment with different SW levels and water inundation times. All the data were subjected to homogeneity test before Turkey's multiple comparison. Statistical analyses were performed in SPSS version 16.0.

3. Results

3.1. Root porosity of S. alterniflora treated with different SW levels and waterlogging times

The root porosity increased with increasing SW level (Fig. 2A) and waterlogging time. The root porosity significantly differed between treatments with 0 + 10SW and 12 h + 10SW (Fig. 2B). Under prolonged waterlogging treatment (i.e., 12 h + 10SW), the plant showed victim symptoms, as indicated by leaf wilting and root necrosis.

3.2. Formation of IP on the root surface of S. alterniflora

The IP content significantly increased with increasing of SW level. The IP content in different SW treatment groups was twice as high as that in the control (Fig. 3A). However, the IP content was not significantly different among SW treatments (Fig. 2A). Under the combined treatment of waterlogging and SW, the highest IP content was observed under the treatment with the shortest waterlogging time and SW level (0 h + 10SW). The IP content decreased with increasing waterlogging time (Fig. 3B). The IP content in the root of plants treated with prolonged waterlogging (8 h + 10SW and 12 h + 10SW) declined to the levels of the control (3.4373 mg g^{-1} DW). The formation of IP on the surface and transverse section of the *S. alterniflora* root were visualized with SEM-EDX (Fig. 3C). The EDX map of the transverse section showed the amount of IP formed under the control treatment was significantly lower than that under SW treatment. The root cells were

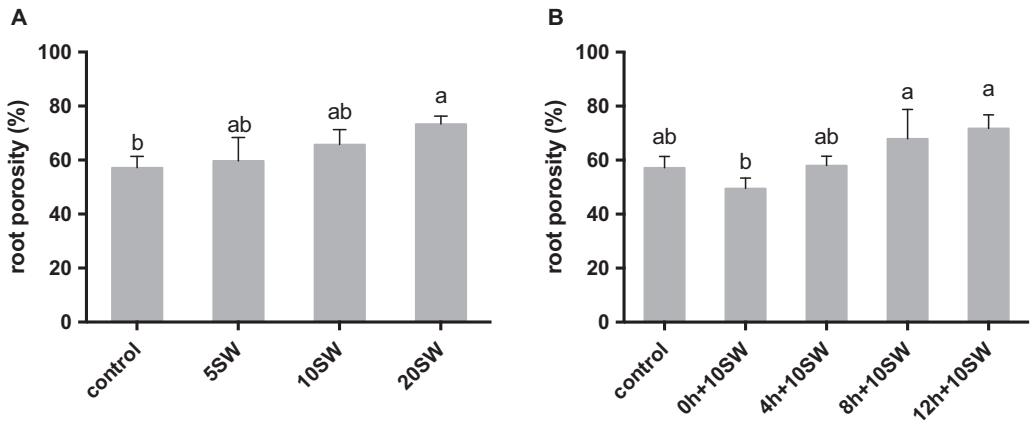

Fig. 2. Changes of root porosity of *S. alterniflora* under (A) different levels of SW treatments and (B) different waterlogging time treatment with SW (values are mean and SD; for each parameter, data with different letters are significantly different at $P \leq 0.05$).

discernible with little sign of deformation (Fig. 3C). The roots of *S. alterniflora* under the 5SW treatment showed relatively higher IP deposition than that under the control probably because of the collapse of outer tangential cell walls (Fig. 3C). The highest level of IP deposition was observed in the treatment with the highest SW level (20SW), and the root surface exhibited serious shrinkage and deformation (Fig. 3C). IP mainly precipitated on the root surface of *S. alterniflora* mainly as amorphous phase but rarely as crystalline phase (Figs. S1A and 1B). The EDX analysis on the root surface of *S. alterniflora* showed that the amorphous and crystalline phases of IP were mainly composed of Fe-rich compounds (Fig. S1). HMs including Cu, Zn, Pb, and Cr did not show any obvious correlations with Fe on the root surface of *S. alterniflora* under the 5SW treatment (Fig. S1).

3.3. Changes in ethylene content and ADH activity in the root

ADH is the main enzyme involved in the detoxification of ethanol in plants under anaerobic waterlogging conditions. The ADH activity in the root of *S. alterniflora* was significantly enhanced in the treatment with low SW levels (5SW) and returned to the control levels after treatment with high SW levels (i.e., 10SW and 20SW; Fig. 4A). The root ADH activity increased with prolonged waterlogging at the same strength of SW (10SW). The ADH activity significantly increased in the treatments with the highest SW level and waterlogging time (12 h + SW, Fig. 4B). Increasing the SW level did not show any stimulatory effect on the ethylene content in the roots of *S. alterniflora* (Fig. 4C). However, the ethylene content increased significantly with increasing waterlogging time (Fig. 4D).

3.4. Content of HMs in plant tissue and IP

Increasing the SW concentrations significantly enhanced the accumulation and translocation of all HMs in the leaves and roots of *S. alterniflora* but did not significantly affect the concentrations of HMs in the DCB solution (IP extract, Fig. 5). In specific, the concentrations of Cu, Pb, and Cr in the leaves and roots significantly increased with increasing SW concentration ($P < 0.001$), but the changes in the contents of these HMs in the DCB extract were not significantly different from those in the control (Fig. 5A). However, the Zn concentration in the DCB extract varied significantly with SW treatment and significantly increased after treatment with the highest SW level (Fig. 5B). These results were supported by the EDX analysis on element composition in the roots under 20SW treatment. Among all HMs, Fe and Zn showed significant accumulation in the surface layer of the *S. alterniflora* root (Fig. S1 in the Supplementary materials). At low levels of SW (5SW and 10SW), the concentrations of different HMs in the roots were higher than those in the leaves. However, at the highest level of SW (20SW), the leaves of *S. alterniflora* had significantly higher concentration of Cu, Zn, and Cr than the roots ($P < 0.05$). All four metals increasingly accumulated in the leaves with increasing SW level.

Under treatment with the same strength of SW and different waterlogging times, the accumulation of all HMs in the leaves of *S. alterniflora* were the highest under treatments with 4 h + 10SW and 8 h + 10SW; the concentrations returned to the control level under shorter (0 h + 10SW) or longer waterlogging time (12 h + 10SW, Fig. 6). The accumulation of HMs in the roots of *S. alterniflora* under 0 h + 10SW was comparable with that in the control. Increasing the waterlogging time significantly enhanced the accumulation of Cu, Zn, and Cr in the root of *S. alterniflora* (Fig. 6). Metals that accumulated in IP were evaluated by measuring their concentrations in the DCB extract. The concentrations of Cu, Zn, and Cr in the DCB extract were the highest under 0 h + 10SW treatment; their concentrations in the DCB extract were significantly higher than those in the leaves and roots ($P < 0.05$). Increasing the waterlogging time decreased the concentrations of Cu, Zn, and Cr in the DCB extract, and such concentrations were lower than those in the roots (Fig. 6A, B, and D).

3.5. Changes in the contents of N and P in plant tissues under SW and waterlogging treatments

Based on the one-way ANOVA, the N content in the leaves of *S. alterniflora* decreased with increasing SW levels. Multiple comparisons indicated that the N content in the leaves was not significantly different among SW treatments; however, the root N content was not affected by SW treatment (Fig. 7A and B). The P concentration in the root of *S. alterniflora* significantly increased with increasing SW level (Fig. 7C) and prolonged waterlogging (Fig. 7D). In the leaves, the P content decreased significantly with increasing waterlogging time, and the lowest level was observed under treatment with 12 h + 10SW (Fig. 7D).

4. Discussion

The formation of IP in wetland plants is mainly induced by O_2 release, porewater Fe^{2+} oxidation, and iron oxide precipitation on the root surface (Armstrong et al., 1992). The availability of O_2 and Fe^{2+} in the rhizosphere sediments are considered as two major limiting factors (Taylor et al., 1984). In the present study, the IP concentration in the root of *S. alterniflora* increased uniformly among different SW treatments compared with that in the control group, and the root porosity significantly increased (Figs. 2 and 3). Hence, SW treatment promoted the formation of IP possibly by increasing root porosity. This result is consistent with those presented in previous studies. Wetland plants with high root porosity and ROL tend to form Fe/Mn plaque (Yang et al., 2014). Increasing the SW concentration increased the contents of

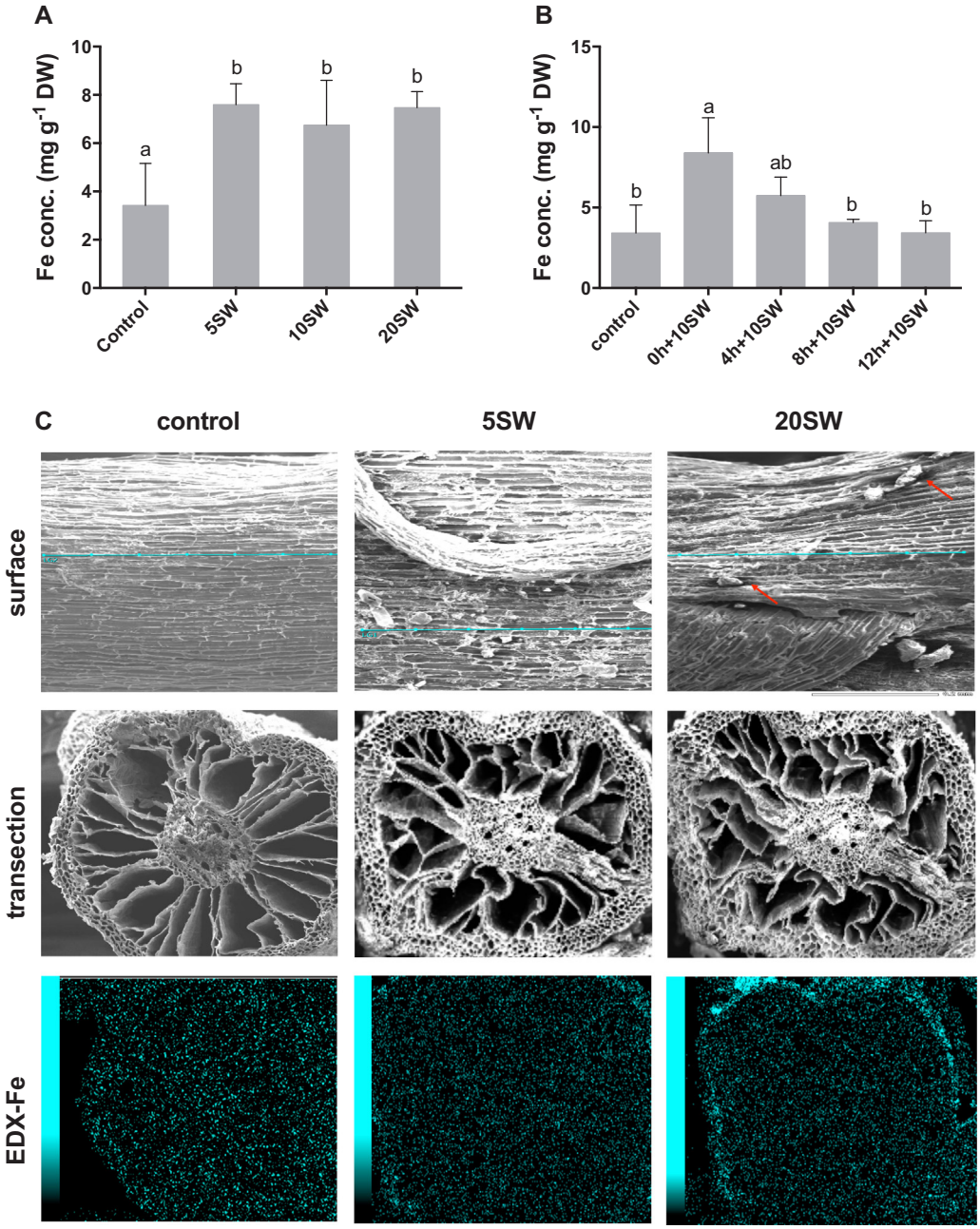

Fig. 3. IP concentration in roots *S. alterniflora* under (A) Different levels of SW treatments and (B) different waterlogging time treatment with SW (values are mean and SD; data with different letters are significantly different at $P \leq 0.05$); (C) the SEM observation of the surface (the top row), transection (the middle row) of the root of S. alterniflora and the energy dispersive X-ray microanalysis of Fe of the root transection (the bottom row).

HMs and organic matter, which might aggravate reduction in the redox potential of the sediments and the porosity of the root, leading to an increase in the amount of oxygen in the root (Pi et al., 2011). In the present study, the amount of IP formed was not significantly different among SW groups probably because of the same Fe^{2+} concentration in the culture medium; moreover, the root porosity did not vary significantly among different SW treatments. Increasing the SW level also introduced P and N into the substrate. According to a previous study, a P-rich environment might inhibit the formation of IP on the root surface (Cheng et al., 2012; Khan et al., 2016). With increasing of the SW level, the P content in the culture substrate increased which might offset the influences of the increased root porosity on IP formation. Mei et al. (2014) found that wastewater treatment significantly induced IP formation in the roots of six wetland species but decreased the rates of ROL and root porosity.

In wetland plants, aerenchyma is formed constitutively, and the formation can be induced under waterlogging conditions (Yamauchi et al., 2018). In the present study, increasing the waterlogging time in treatments with the same strength of SW increased the root porosity (more aerenchyma tissues) in *S. alterniflora*. The root porosity under treatment with 12 h + 10SW was significantly higher than that under treatment with the shortest waterlogging time (0 h + 10SW). However, the highest amount of IP was formed under treatment with 0 h + 10SW (Fig. 3). Previous studies showed that the aeration conditions of the sediments and the oxidizing capacity of the plant roots can influence the formation of IP in the roots of wetland plants (Cheng et al., 2010; Xu et al., 2018). Our previous study also showed that *S. alterniflora* possessed the highest amount of IP formed under the shortest waterlogging time (3 h per day) with HM treatment; the formation of IP generally decreased with increasing waterlogging time (Xu et al., 2018). These

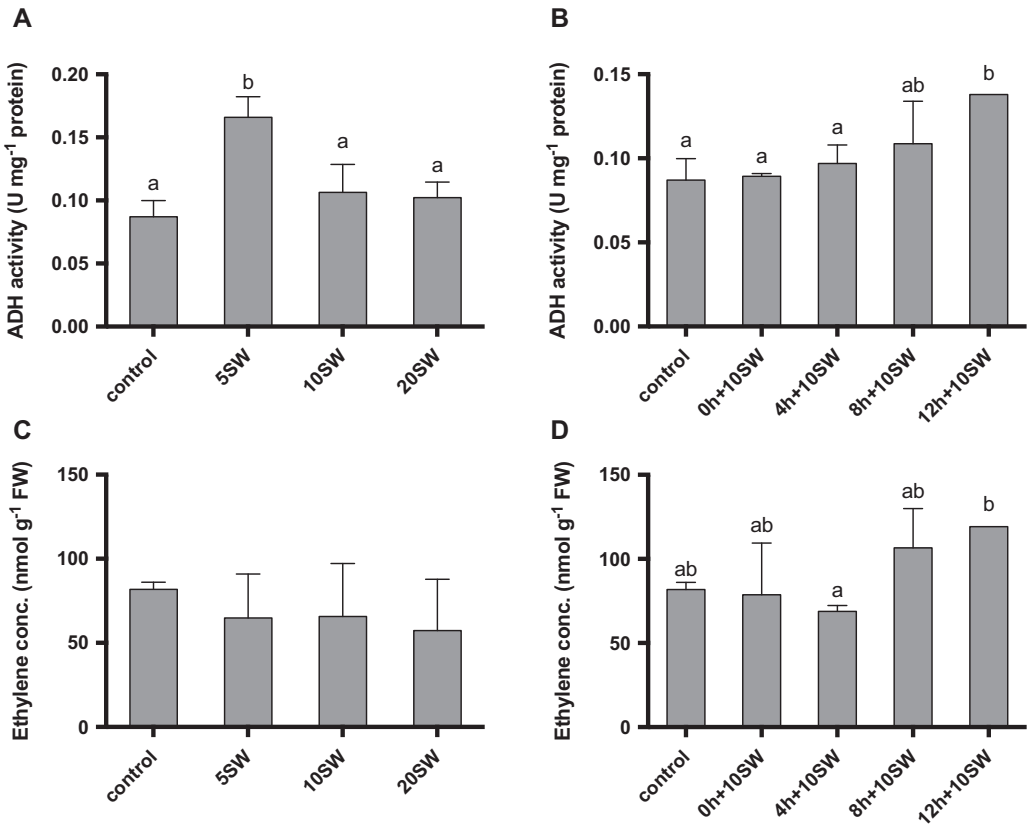

Fig. 4. Changes of ADH activity and ethylene content in root of *S. alterniflora* under different levels of SW treatments (A&C) and different waterlogging time treatment with SW (B&D) (values are mean and SD; data with different letters are significantly different at P ≤ 0.05; no letter appended if the data were not significantly different).

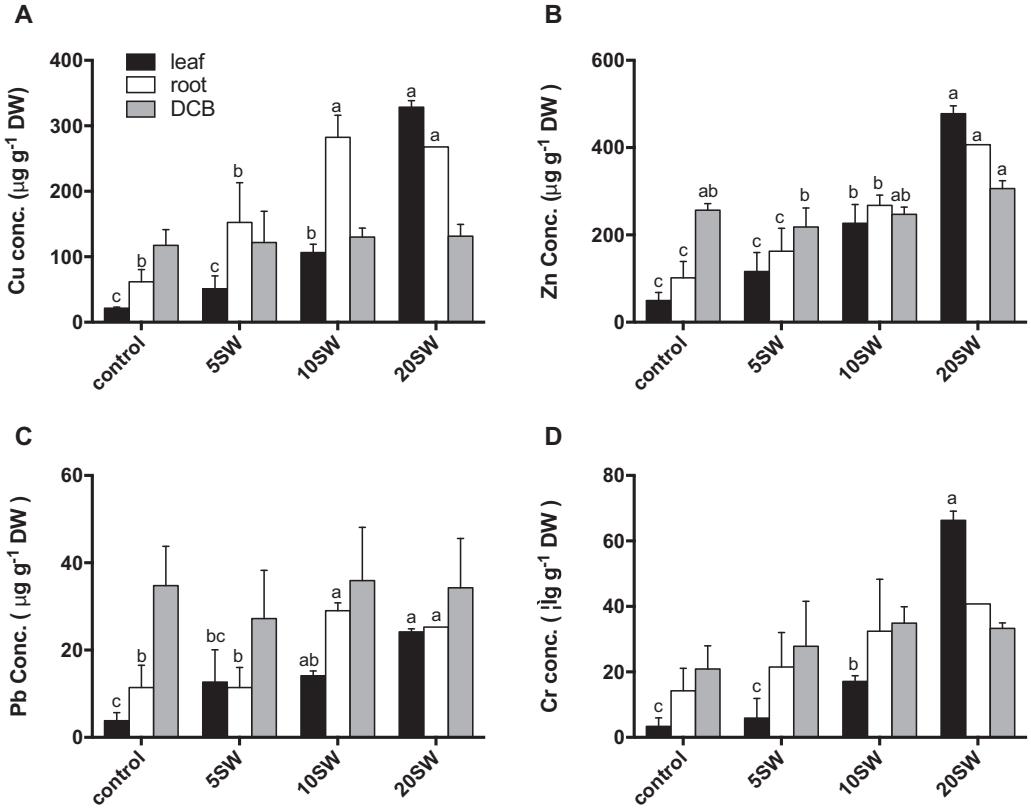

Fig. 5. The accumulations of (A) Cu, (B) Zn, (C) Pb and (D) Cr in roots, leaves and root DCB extract of *S. alterniflora* under different levels of SW treatments (values are mean and SD; data with different letters are significantly different at P ≤ 0.05; no letter appended if the data were not significantly different).

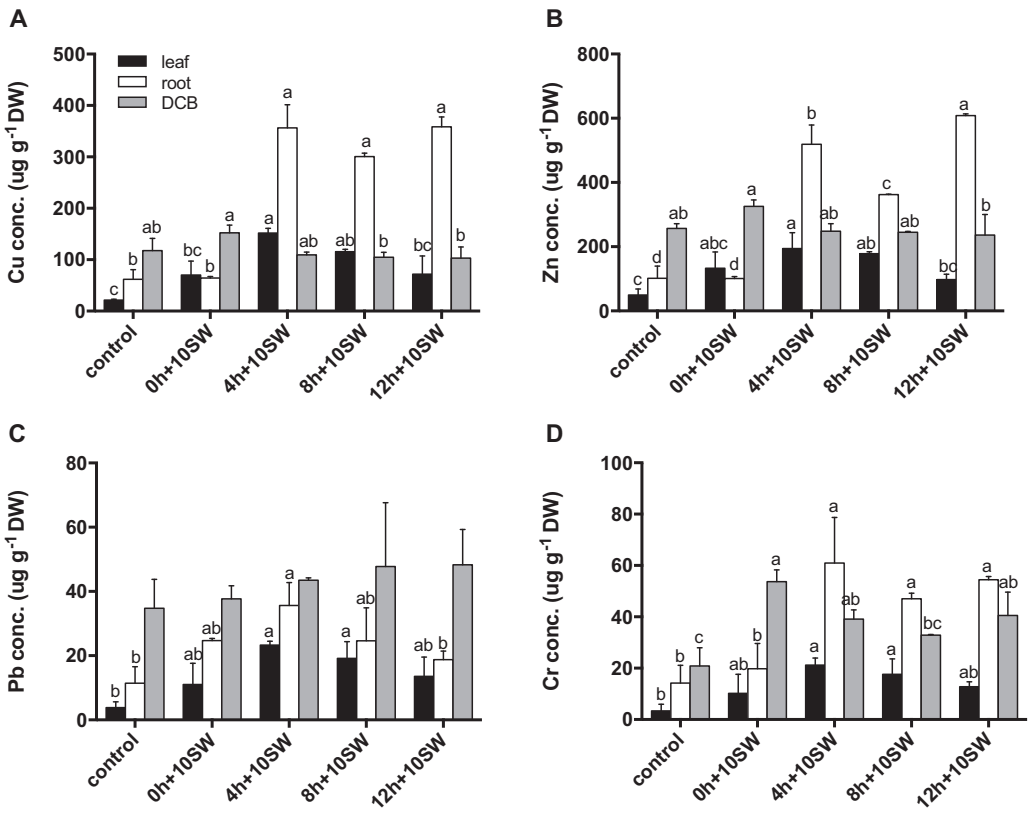

Fig. 6. The accumulations of (A) Cu, (B) Zn, (C) Pb and (D) Cr in roots, leaves and root DCB extract of *S. alterniflora* under different waterlogging time treatment with SW (values are mean and SD; data with different letters are significantly different at $P \leq 0.05$; no letter appended if the data were not significantly different).

results could be attributed to the fact that the rhizosphere of the plants under 0 h + 10SW treatment is more oxic than those under treatment with long waterlogging time; the more oxic nature of sediments favored the oxidation of Fe^{2+} and the formation of IP. With increasing waterlogging time, the formation of IP was inhibited despite the significant increase in the root porosity. This finding could be due to the necrosis of root tissues under prolonged waterlogging with SW treatment (i.e., 12 h + 10SW). Root porosity is mainly derived from the development of aerenchyma tissues in the roots of wetland plants; the development of the aerenchyma is mainly induced by lysigeny (cell death and dissolution), which is controlled by internal and external stimuli, such as hypoxia and ethylene (Takahashi et al., 2014; Yamauchi et al., 2018). In the present study, the ethylene content in the roots of *S. alterniflora* increased significantly with increasing waterlogging time because of root tissue necrosis and hypoxia. *S. alterniflora* treated under prolonged waterlogging showed apparent victim symptoms, such as leaf wilting and root necrosis, which could aggravate the transportation of oxygen from the above-ground plant parts to the below-ground part; this phenomenon leads to the decreased root ROL of the plants. In general, hypoxia due to waterlogging stress may enhance ethylene synthesis. The increase in the ethylene content can upregulate the activity of cellulase, which accelerates the separation and decomposition of the cytoplasm and the development of aerenchyma tissues (Yin et al., 2013). In the present study, the increase in the root porosity with increasing waterlogging time may lead to the increase in the ethylene concentration in the roots of *S. alterniflora*.

Ethanol toxicity is a primary cause of injury and death in plants under flooding conditions (Maricle et al., 2014). ADH, which is the major enzyme produced by plants under anaerobic waterlogging conditions, can catalyze the conversion of toxic ethanol into acetaldehyde and help plant roots avoid ethanol damage caused by hypoxia (Wang and Zhang, 2001). Maricle et al. (2014) found that flood-tolerant species, such as *S. alterniflora*, *Spartina patens*, and *Phragmites australis*, are more tolerant to ethanol toxicity than flood-sensitive species. In the present study, increasing the waterlogging time significantly increased the root ADH activity, ethylene production, and aerenchyma tissue development. Hence, *S. alterniflora* exhibited a certain degree of tolerance to hypoxic conditions. Pezeshki et al. (1993) found a close relationship between root hypoxia and increase in ADH activity, ethylene production, and aerenchyma tissue development in *S. patens*; the enhanced ADH activity and ethylene production in plants subjected to hypoxia have adaptive significance for plants under hypoxic conditions. The high ADH activity indicated that the aerenchyma in the roots of *S. alterniflora* cannot sufficiently provide the required amount of oxygen for aerobic respiratory demand. Mendelssohn et al. (1981) suggested that the aerenchyma tissue in *S. alterniflora* can only provide sufficient oxygen to the roots for predominately aerobic respiration in moderately, but not highly, reduced substrates. The transplantation of streamside *S. alterniflora* swards into the more waterlogged and less productive inland marshes caused rapid decreases in the soil redox potential and increases in the root ADH activity (Mendelssohn and Mckee, 1988).

IP can bind to HMs and nutrient elements by adsorption and co-precipitation and thus affects their accumulation and transportation in plants (Khan et al., 2016). However, the precise effect of IP on the absorption of trace metals and nutrients is inconclusive. Opposing views have been proposed, that is, IP on the root surface can prevent or promote the absorption of HMs and nutrient elements (Zhang et al., 1999; Ye et al., 2001; Thakur et al., 2016). In the present study, increasing the SW level did not increase the accumulation of HMs in the DCB extract but increased the amount of IP formed. Hence, the increase in HM accumulation in *S. alterniflora* followed a dose-dependent pattern and might be irrelevant to IP formation in the roots. However, the results of the waterlogging experiment showed that HMs that accumulated in the DCB extract was substantially proportional to the concentration of IP in the root. The formation of IP under nonwaterlogging

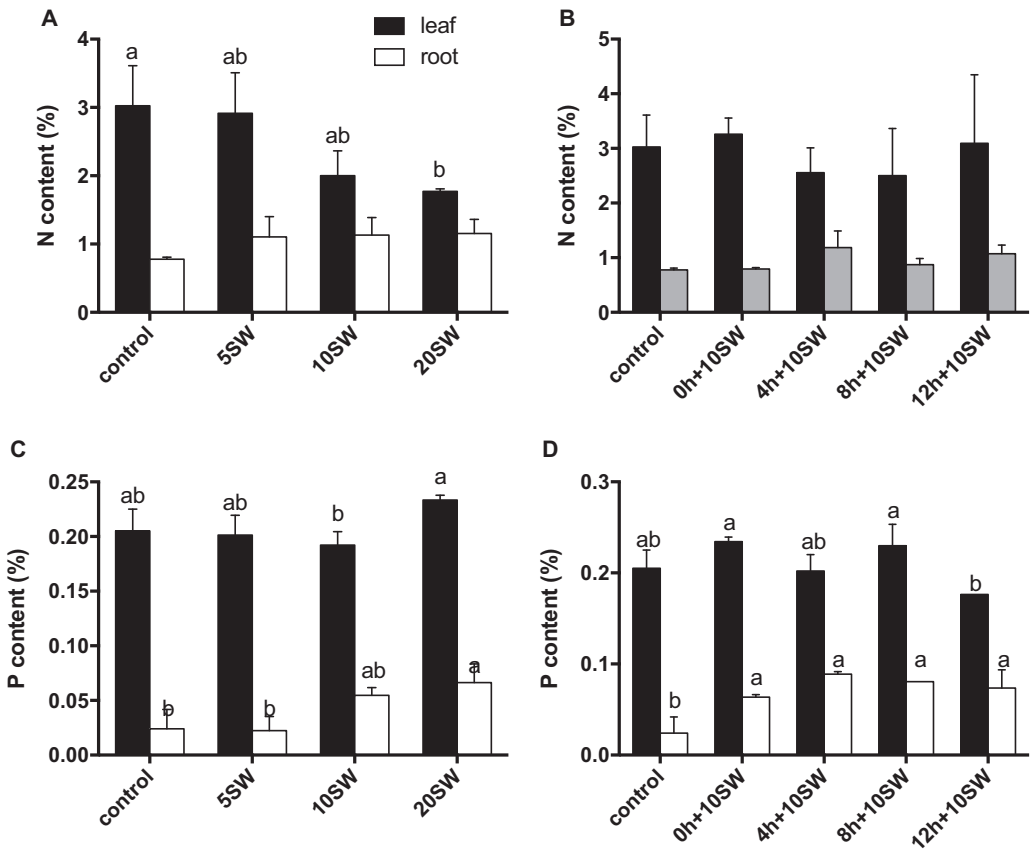

Fig. 7. N (A&B) and P (C&D) contents in roots and leaves of *S. alterniflora* under different levels of SW treatments and different waterlogging time treatment with SW (values are mean and SD; data with different letters are significantly different at P ≤ 0.05; no letter appended if the data were not significantly different).

conditions (i.e. 0 h + 10SW) might favor the accumulation of HMs in IP; the accumulation of HMs in the roots and leaves of *S. alterniflora* was significantly inhibited compared with that under prolonged waterlogging (Fig. 6). The SEM-EDX analysis also revealed that IP formed on the surface (either amorphous or crystalline phase) of *S. alterniflora* absorbed HMs such as Cu, Zn, and Cr (Fig. S1). The highest amount of IP formed under SW and waterlogging treatments was more or less comparable, but the effect of these treatments on HM absorption was different. These two contradictory results imply that the function of IP on the absorption of HMs is dependent on the aerobic/anaerobic condition of the sediments. The waterlogging conditions considerably influence the availability of HMs in the sediments (Calvo-Cubero et al., 2016). With increasing waterlogging time, the sediment redox potential decreased, and insoluble Fe^{3+} and $Mn^{3+/4+}$ (hydr) oxides were reduced into soluble Fe^{2+} and Mn^{2+}; this phenomenon led to release of the absorbed HMs to sediment porewater and increase in the bioavailability of HMs in plants. Therefore, the uptake of HMs by plants was significantly enhanced under long waterlogging time (Fig. 6). The sediments in the 0 h + 10SW treatment are more oxic than those under waterlogging treatments. More metal ions were immobilized by trivalent Fe/Mn (hydr)oxides through coprecipitation or adsorption, and the uptake of these metals was restrained. The precise role of IP in the uptake of HMs by plants may be regulated by sediment physiochemical conditions, such pH. Batty et al. (2000) suggested that IP formed in the roots of *P. australis* may impede the uptake of Cu to the shoot under high pH condition (6.0); this effect will be masked by H^+ ions under low pH condition (3.5). In estuarine wetlands, the pH of acid sulfate sediments usually decreased with increasing flooding time (Michalcová et al., 2011). We could hypothesize that the relatively long waterlogging time in the present study (i.e., 8 h + 10SW and 12 h + 10SW) made the sediments to be more acidic than treatment without waterlogging and led to impaired HM absorption into IP.

In this study, increasing the SW level increased the accumulation of P in the leaves and roots of *S. alterniflora* but did not significantly affect N content. Treatment with increased waterlogging time but the same strength of SW enhanced P accumulation in the roots. The increased uptake of P in the roots and leaves of *S. alterniflora* might enhance IP formation in the roots. These results are consistent with those in previous studies. Hence, IP might enhance the accumulation of P in the below- and/or above-ground parts of rice (*Oryza sativa* L.) (Zhang et al., 1999) or other wetland plants, such as *Pilea cadierei* (Yang et al., 2011) and *T. latifolia* (Cao et al., 2013). The underlying mechanism for the improved nutrient uptake remains unclear. A possible mechanism is that P can be exchanged or form a complex with OH groups in IP, which will be a P reservoir, thereby enhancing the diffusion of P into the roots of the wetland plant and increasing the P concentration in the shoots (Zhang et al., 1999; Xu et al., 2009; Khan et al., 2016). The decrease in the N content in the leaves may be induced by high wastewater concentration, which could hinder the synthesis of organic compounds in the leaves.

5. Conclusion

This study revealed that the amount of IP formed in the root of *S. alterniflora* increased with increasing SW level under periodic waterlogging for 8 h per day. The enhanced formation of IP under the SW treatment could be attributed to the increase in the root porosity. At a fixed SW level, the formation of IP in the root of *S. alterniflora* was inhibited by increasing the waterlogging time, but the root porosity increased significantly. Increasing the SW level did not enhance the accumulation of HMs in the DCB extract. The increase in the HM accumulation in *S. alterniflora* followed a dose-dependent pattern. The

highest amount of IP formed under treatment with the highest SW level and nonwaterlogging condition was more or less comparable, but their effect on HM absorption was different. Based on the experiment with different waterlogging times, the amount of HMs that accumulated in the DCB extract was substantially proportional to the concentration of IP in the root. The presence of IP under nonwaterlogging conditions (i.e. 0 h + 10SW) favored the accumulation of HMs in IP. The accumulation of HMs in the roots and leaves of *S. alterniflora* was significantly inhibited compare with that under prolonged waterlogging treatment. The SEM-EDX analysis also revealed that IP formed in *S. alterniflora* could absorb HMs and affect their translocation in plants. The present study validated some results of our previous study that long-time water inundation did harm to the health of *S. alterniflora* while favored the stabilization and accumulation of HMs in the sediments and in plants (Sun et al., 2018), and further revealed that appropriated water inundation time favored the formation of IPs and the accumulation of HMs in roots and leaves of S. alterniflora, and should be considered in the construction of artificial wetlands for wastewater treatment. The actual effect of IP on HM and nutrients translocation under aerobic/anaerobic condition should be further investigated,

Acknowledgements

The work described in this paper was supported by Natural Science Foundation of Shanghai, China (16ZR1410300), Independent Research Foundation of State Key Laboratory of Estuarine and Coastal Research, China (2016RCPY01) and National Natural Science Foundation of China (41877413).

Appendix A. Supporting information

Supplementary data associated with this article can be found in the online version at doi:10.1016/j.ecoenv.2018.10.072.

References

Anjum, N.A., Ahmad, I., Valega, M., Mohmood, I., Gill, S.S., Tuteja, N., Duarte, A.C., Pereira, E., 2014. Salt marsh halophyte services to metal–metalloid remediation: assessment of the processes and underlying mechanisms. Crit. Rev. Environ. Sci. Technol. 44 (18), 2038–2106.
Armstrong, J., Armstrong, W., Beckett, P.M., 1992. *Phragmites australis*: venturi-and humidity-induced pressure flows enhance rhizome aeration and rhizosphere oxidation. New Phytol. 120, 197–207.
Batty, L.C., Baker, A.J.M., Wheeler, B.D., Curtis, C.D., 2000. The effect of pH and plaque on the uptake of Cu and Mn in *Phragmites australis* (cav.) trin ex. steudel. Ann. Bot. 86 (3), 647–653.
Calvo-Cubero, J., Ibáñez, C., Rovira, A., Sharpe, P.J., Reyes, E., 2016. Changes in water and soil metals in a mediterranean restored marsh subject to different water management schemes. Restor. Ecol. 24 (2), 235–243.
Cao, X.Y., Chong, Y.X., Yu, G.W., Zhong, H.T., 2013. The role of root iron plaque in phosphorus removal of constructed wetland and the effect of medium on iron plaque. Acta Sci. Circumst. 33 (5), 1292–1297.
Chai, C., Yu, Z., Song, X., Cao, X., 2006. The status and characteristics of eutrophication in the Yangtze river (Changjiang) estuary and the adjacent East China Sea, China. Hydrobiologia 563 (1), 313–328.
Chai, M., Shi, F., Li, R., Liu, L., Liu, Y., Liu, F., 2013. Interactive effects of cadmium and carbon nanotubes on the growth and metal accumulation in a halophyte *Spartina alterniflora* (Poaceae). Plant Growth Regul. 71 (2), 171–179.
Cheng, H., Liu, Y., Tam, N.F.Y., Wang, X., Li, S.Y., Chen, G.Z., Ye, Z.H., 2010. The role of radial oxygen loss and root anatomy on zinc uptake and tolerance in mangrove seedlings. Environ. Pollut. 158, 1189–1196.
Cheng, H., Tam, N.F.Y., Wang, Y., Li, S., Chen, G., Ye, Z., 2012. Effects of copper on growth, radial oxygen loss and root permeability of seedlings of the mangroves *Bruguiera gymnorrhiza* and *Rhizophora stylosa*. Plant Soil 359 (1–2), 255–266.
Chibuike, G.U., Obiora, S.C., 2014. Heavy metal polluted soils: effect on plants and bioremediation methods. Appl. Environ. Soil Sci. 2014, 243–254.
Duarte, D.H., Shinzato, P., dos Santos Gusson, C., Alves, C.A., 2015. The impact of vegetation on urban microclimate to counterbalance built density in a subtropical changing climate. Urban Clim. 14, 224–239.
Jackson, M.B., Armstrong, W., 1999. Formation of aerenchyma and processes of plant ventilation in relation to soil flooding and submergence. Plant Biol. 1, 274–287.
Jensen, C.R., Luxmoore, R.J., Vangundy, S.D., Stolzy, L.H., 1969. Root air measurements by a pycnometer method. Agron. J. 61 (3), 474–475.
Khan, N., Seshadri, B., Bolan, N., Saint, C.P., Kirkham, M.B., Chowdhury, S., Yamaguchi, N., Lee, D.Y., Li, G., Kunhikrishnan, A., Qi, F., Karunanithi, R., Qiu, R., Zhu, Y.G., Syu, C.H., 2016. Root iron plaque on wetland plants as a dynamic pool of nutrients and contaminants. Adv. Agron. 138, 1–96.
Lee, C.H., Hsieh, Y.C., Lin, T.H., Lee, D.Y., 2013. Iron plaque formation and its effect on arsenic uptake by different genotypes of paddy rice. Plant Soil 363, 231–241.
Maricle, B.R., White, S.J., Meraz, A., Maforo, N.G., Biggs, T.N., Martin, N.M., Caudle, K.L., 2014. Effect of ethanol toxicity on enzyme activity in anaerobic respiration in plants. Trans. Kansas Acad. Sci. 237–244.
Mei, X.Q., Yang, Y., Tam, N.F., Wang, Y.W., Li, L., 2014. Roles of root porosity, radial oxygen loss, Fe plaque formation on nutrient removal and tolerance of wetland plants to domestic wastewater. Water Res. 50 (3), 147–159.
Mendelssohn, I.A., Mckee, K.L., 1988. *Spartina alterniflora* die-back in Louisiana: time-course investigation of soil waterlogging effects. J. Ecol. 76 (2), 509–521.
Mendelssohn, I.A., Mckee Jr, K.L., P.W, 1981. Oxygen deficiency in *Spartina alterniflora* roots: metabolic adaptation to anoxia. Science 214 (4519), 439–441.
Michalcová, D., Gilbert, J.C., Lawson, C.S., Gowing, D.J.G., Marrs, R.H., 2011. The combined effect of waterlogging, extractable P and soil pH on α-diversity: a case study on mesotrophic grasslands in the UK. Plant Ecol. 212 (5), 879–888.
Otte, M.L., Rozema, J., Koster, L., Haarsma, M.S., Broekman, R.A., 1989. Iron plaque on roots of *Aster tripolium* L.: interaction with zinc uptake. New Phytol. 111 (2), 309–317.
Pezeshki, S.R., Pardue, J.H., DeLaune, R.D., 1993. The influence of soil oxygen deficiency on alcohol dehydrogenase activity, root porosity, ethylene production and photosynthesis in *Spartina patens*. Environ. Exp. Bot. 33 (4), 565–573.
Pi, N., Tam, N.F., Wong, M.H., 2011. Formation of iron plaque on mangrove roots receiving wastewater and its role in immobilization of wastewater-borne pollutants. Mar. Pollut. Bull. 63 (5–12), 402–411.
Sebastian, A., Prasad, M.N., 2016. Iron plaque decreases cadmium accumulation in *Oryza sativa* L. and serves as a source of iron. Plant Biol. 18 (6), 1008–1015.
Shimamura, S., Mochizuki, T., Nada, Y., Fukuyama, M., 2003. Formation and function of secondary aerenchyma in hypocotyl, roots and nodules of soybean (*Glycine max*) under flooded conditions. Plant Soil 251 (2), 351–359.
Smith, K.E., Luna, T.O., 2013. Radial oxygen loss in wetland plants: potential impacts on remediation of contaminated sediments. J. Environ. Eng. 139 (4), 496–501.
Striker, G.G., 2012. Flooding stress on plants: anatomical, morphological and physiological responses. Botany.
Sun, X., Xu, Y., Zhang, Q., Li, X., Yan, Z., 2018. Combined effect of water inundation and heavy metals on the photosynthesis and physiology of *Spartina alterniflora*. Ecotoxicol. Environ. Saf. 153, 248–258.
Takahashi, H., Yamauchi, T., Colmer, T.D., Nakazono, M., 2014. Aerenchyma formation in plants. In: van Dongen, J.T., Licausi, F. (Eds.), Low-Oxygen Stress in Plants. Springer, Vienna, pp. 247–265.
Taylor, G.J., Crowder, A.A., Rodden, R., 1984. Formation and morphology of an iron plaque on the roots of *Typha latifolia* L. grown in solution culture. Am. J. Bot. 71 (5), 666–675.
Taylor, G.J., Crowder, A.A., 1983. Uptake and accumulation of heavy metals by *Typha latifolia* in wetlands. Can. J. Bot. 61 (1), 63–73.
Thakur, S., Singh, L., Wahid, Z.A., Siddiqui, M.F., Atnaw, S.M., Din, M.F.M., 2016. Plant-driven removal of heavy metals from soil: uptake, translocation, tolerance mechanism, challenges, and future perspectives. Environ. Monit. Assess. 188, 206–212.
Tsang, S., Phu, F., Baum, M.M., Poskrebyshev, G.A., 2007. Determination of phosphate/arsenate by a modified molybdenum blue method and reduction of arsenate by $S_2O_4^{2-}$. Talanta 71 (4), 1560–1568.
Wang, H., Wang, J., Liu, R., Yu, W., Shen, Z., 2015. Spatial variation, environmental risk and biological hazard assessment of heavy metals in surface sediments of the Yangtze River estuary. Mar. Pollut. Bull. 93 (1–2), 250–258.
Wang, W.Q., Zhang, F.S., 2001. The physiological and molecular mechanism of adaptation to anaerobiosis in higher plants. Plant Physiol. Commun. 37, 63–70.
Weis, J.S., Weis, P., 2004. Metal uptake, transport and release by wetland plants: implications for phytoremediation and restoration. Environ. Int. 30 (5), 685–700.
Xu, D., Xu, J.M., He, Y., Huang, P.M., 2009. Effect of iron plaque formation on phosphorus accumulation and availability in the rhizosphere of wetland plants. Water Air Soil Poll. 200 (1–4), 79–87.
Xu, Q.T., Fan, H.Y., Jiang, Z., Zhou, Z.Q., Yang, L., Mei, F.Z., Qu, L.H., 2013. Cell wall degradation and the dynamic changes of Ca^{2+} and related enzymes in the developing aerenchyma of wheat (*Triticum aestivum* L.) under waterlogging. Acta Biol. Hung. 64, 328–340.
Xu, Y., Sun, X., Zhang, Q., Li, X., Yan, Z., 2018. Iron plaque formation and heavy metal uptake in *Spartina alterniflora* at different tidal levels and waterlogging conditions. Ecotoxicol. Environ. Safe 153, 91–100.
Yamauchi, T., Colmer, T.D., Pedersen, O., Nakazono, M., 2018. Regulation of root traits for internal aeration and tolerance to soil waterlogging-flooding stress. Plant Physiol. 176 (2), 1118–1130.
Yang, H., Xie, P., Ni, L., Flower, R.J., 2012. Pollution in the Yangtze. Science 337 (6093), 410.
Yang, J., Tam, F.Y., Ye, Z., 2014. Root porosity, radial oxygen loss and iron plaque on roots of wetland plants in relation to zinc tolerance and accumulation. Plant Soil 374 (1–2), 815–828.
Yang, L., Li, Y., Yang, X., Xiao, H., Peng, H., Deng, S., 2011. Effects of iron plaque on phosphorus uptake by *Pilea cadierei* cultured in constructed wetland. Procedia Environ. Sci. 11 (1), 1508–1512.
Ye, Z.H., Whiting, S., Qian, J.H., Lytle, C.M., Lin, Z.Q., Terry, N., 2001. Trace element removal from coal pile leachate by an Alabama 10-year old constructed wetland. J. Environ. Qual. 30, 1710–1719.
Yin, D., Chen, S., Chen, F., Jiang, J., 2013. Ethylene promotes induction of aerenchyma formation and ethanolic fermentation in waterlogged roots of *Dendranthema* spp. Mol. Biol. Rep. 40 (7), 4581–4590.
Zhang, X.K., Zhang, F.S., Mao, D.R., 1999. Effect of iron plaque outside roots on nutrient uptake by rice (*Oryza sativa* L.): phosphorus uptake. Plant Soil 209 (2), 187–192.